

Infrared vibrational spectra of *tert*-butyl halides in low-aluminum H-Y Faujasite: Vibrational excitation exchange and other effects of guest–host interactions

Jack D. Fox *

Research and Development, Rochester Midland Corporation, 333 Hollenbeck Street, Rochester, NY 14621, USA

Received 27 June 2005; accepted 21 December 2005

Available online 3 February 2006

Abstract

Fourier transform infrared (FTIR) studies at 295 K of low-aluminum H-Y (LAHY, Si/Al = 40) faujasite zeolite supercage-included *tert*-butyl halides, (CH₃)₃C–X (X = Cl, Br, I), are presented in comparison with the adsorbate molecular gas-phase and unloaded host solid-state spectra. The FTIR results, aided by computer modeling studies, reveal a propensity toward the exchange of quanta of vibrational excitation between guest modes, and between guest and host modes. The exchange phenomenon and some pseudo-hydrogen bonding effects are related to the siting of the guest molecules in the host supercage, and to the guest–host interactions at the guest site. © 2006 Elsevier B.V. All rights reserved.

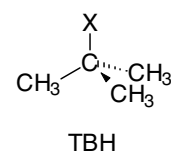
Keywords: Vibrational excitation exchange; Infrared spectrometry; Faujasites; *tert*-Butyl halides

1. Introduction

Dehydrated X- and Y-type faujasite zeolites are very well studied, largely because of their catalytic properties [1]. Modification of zeolite parameters, such as the Si/Al ratio, type of exchangeable cation, or the inclusion of another catalytic agent, can affect the reaction product of an adsorbed species [2]. Zeolite H-Y is available in dealuminated form with very high Si/Al ratio and is also known as siliceous Y. This zeolite is the subject of this work and will be denoted LAHY (low aluminum H-Y). The present work focuses on the interactions between a series of organohalogen guest molecules and the LAHY faujasite host, in which charge-compensating cations play a negligible role. Thus, this study enables one to isolate the framework–guest interactions.

A variety of spectroscopic, calorimetric, adsorption, and modeling studies have been applied to guest-LAHY sys-

tems [3–13]. Only three of these examine organohalogenes [9,11,12]. Two of the studies examine chlorocyclohexanes [11,12] and *n*-hexane [13] by FT-Raman spectroscopy. These studies do not include a



systematic study of halogen variation within a single type of organohalogen molecule, as was done previously in Na-X with the *tert*-butyl halide (TBH) series [14], nor do they constitute a systematic comparison of the organohalide series in LAHY with the series in Na-X, in whose supercages charge-compensating cations are present. It can be said, however, that a unifying theme in these previous LAHY studies is that the site-dependent and orientation-dependent guest–host interactions are generally weaker than is observed in lower Si/Al ratio faujasite zeolites.

* Tel.: +1 585 336 2367; fax: +1 585 336 2306.

E-mail address: jfox@rochestermidland.com.

It is well known that the three basic effects governing the adsorption of guests in faujasites are guest interactions with cations, guest interactions with framework oxygen atoms facing into the supercages, and competitive interactions of these kinds with adsorbed water [14]. A previous FTIR study of the TBH series in dry Na-X showed that the cation–molecule and framework–molecule interactions lead to specific sitings of the guests in the supercage [14]. These sitings were shown often to exhibit characteristic mutual perturbations between guest and host vibrational bands that have proximate frequencies. The relationships between the guest functional group interactions with Na-X and the guest–host vibrational mode effects were often very characteristic of the siting of the guest in Na-X, as determined in companion with molecular modeling studies. Thus, the present FTIR and molecular modeling studies of the adsorbed TBH series in LAHY serve to isolate the effect of guest–framework oxygen interactions from the guest–cation interactions that were present, together with the guest–framework oxygen interactions, in this previous study of the TBH series in Na-X [14].

It will be seen that the weaker framework oxygen–guest interactions, in the absence of supercage cations, give rise to a distinctly different siting in the supercage and a distinctly different pattern of guest–host vibrational mode interactions than were observed for the TBH in Na-X [14]. The weaker interactions in the LAHY host appear to lead to a vibrational mode of the guest molecule interacting with several more-or-less degenerate host modes of comparable frequencies, or with another guest mode, leading to an exchange of quanta of vibrational excitation between guest modes, or between guest and host modes. In the Na-X study [14], where the guest–host interactions were stronger, vibrational interactions appeared to be predominantly between a molecular mode and a single host mode of comparable frequency.

2. Experimental details

Detailed descriptions of experimental aspects, including sample loading [14] and faujasite characterization [15], can be found in the [Supplementary Material](http://www.sciencedirect.com) accompanying this work (<http://www.sciencedirect.com>), and in a previous publication [14].

Commercially available LAHY with Si/Al = 40 (Zeolyst Corp.) was dried by heating in vacuo [14]. The LAHY was loaded by the evaporative transfer of four molecules per supercage of TBH (*tert*-butyl chloride, TBC, *tert*-butyl bromide, TBB, and *tert*-butyl iodide, TBI). FTIR transmission experiments were performed on wafers prepared by the KBr dilution technique [16] at approximately 1% (w/w) of loaded LAHY in KBr. Loaded faujasite samples were handled in the water- and oxygen-scrubbed Ar atmosphere of a glove box. The nominal FTIR spectral resolution of 2 cm^{-1} , taken together with the frequency calibration [17] across the whole recorded band, resulted in overall accuracies of 3 cm^{-1} for wavenumber values and 4 cm^{-1} for

wavenumber shifts [14]. The accuracy of comparisons of proximate peak positions, however, probably approaches the 2 cm^{-1} resolution. Averages of 128 scans were accumulated.

3. Experimental results

Figs. 1–3 display spectra grouped by individual TBH molecule in the gas phase and absorbed into LAHY, in comparison with the spectrum of the unloaded host. The unloaded LAHY IR spectrum has been compared with the Na-X spectrum [14] and with the Al_2O_3 and SiO_2 spectra [18] for the purpose of assigning the host bands. See [Figure 1S and Table 2S in the Supplementary Material \(http://www.sciencedirect.com\)](http://www.sciencedirect.com), where these data, together with calculations on SiOH_4 and AlOH_4^- fragments and the all-silicon (Si-Y) framework, are employed to assign the LAHY bands. Table 1 lists the experimental spectral parameters for the TBH-LAHY guest–host systems. The method of analysis of the band center, $\bar{\nu}_0$, linewidth, $\Delta\bar{\nu}_0$, and intensity, I_0 , parameters were described in a previous publication [14], together with the method of analysis of the uncertainties in the parameters. The guest experimental band assignments given in Table 1 were reported in a previous publication [14], where diagrams of the guest vibrational normal mode displacements may also be found.

In general the guest mode linewidths are decreased upon loading into LAHY relative to their gas phase values, except in a few cases where several modes cluster, i.e. $\{v_4, v_{18}\}$ and $\{v_3, v_{16}, v_{17}\}$. The relative intensity behavior is complex with few recognizable trends.

Following, descriptions of the guest and host band positions on a band-by-band basis are presented. Expanded views of the regions discussed here may be found in both this manuscript and the [Supplementary Material \(http://www.sciencedirect.com\)](http://www.sciencedirect.com), where the host band assignments are also described in detail.

3.1. C–X stretching, v_7

The positions of the TBH gas-phase v_7 bands are located at 584 cm^{-1} (TBC), 525 cm^{-1} (TBB), and 495 cm^{-1} (TBI). The bridging oxygen atom (BOA) band of unloaded LAHY lies at 532 cm^{-1} . Upon loading the guest into the host, what remains are single peaks located near the host BOA band at 528 cm^{-1} (TBC), 529 cm^{-1} (TBB), and 529 cm^{-1} (TBI). Fig. 4 presents an expanded view of the coalescence between the TBB C–Br stretching vibrational mode v_7 and the LAHY band arising from D6R/S4R BOA vibrational modes, as well as of the isolated guest and host bands that participate.

3.2. C–C and C–X stretching, v_6

The positions of the *tert*-butyl halide gas phase v_6 bands are located at 816 cm^{-1} (TBC), 808 cm^{-1} (TBB), and 805 cm^{-1} (TBI). The frequencies of these guest bands,

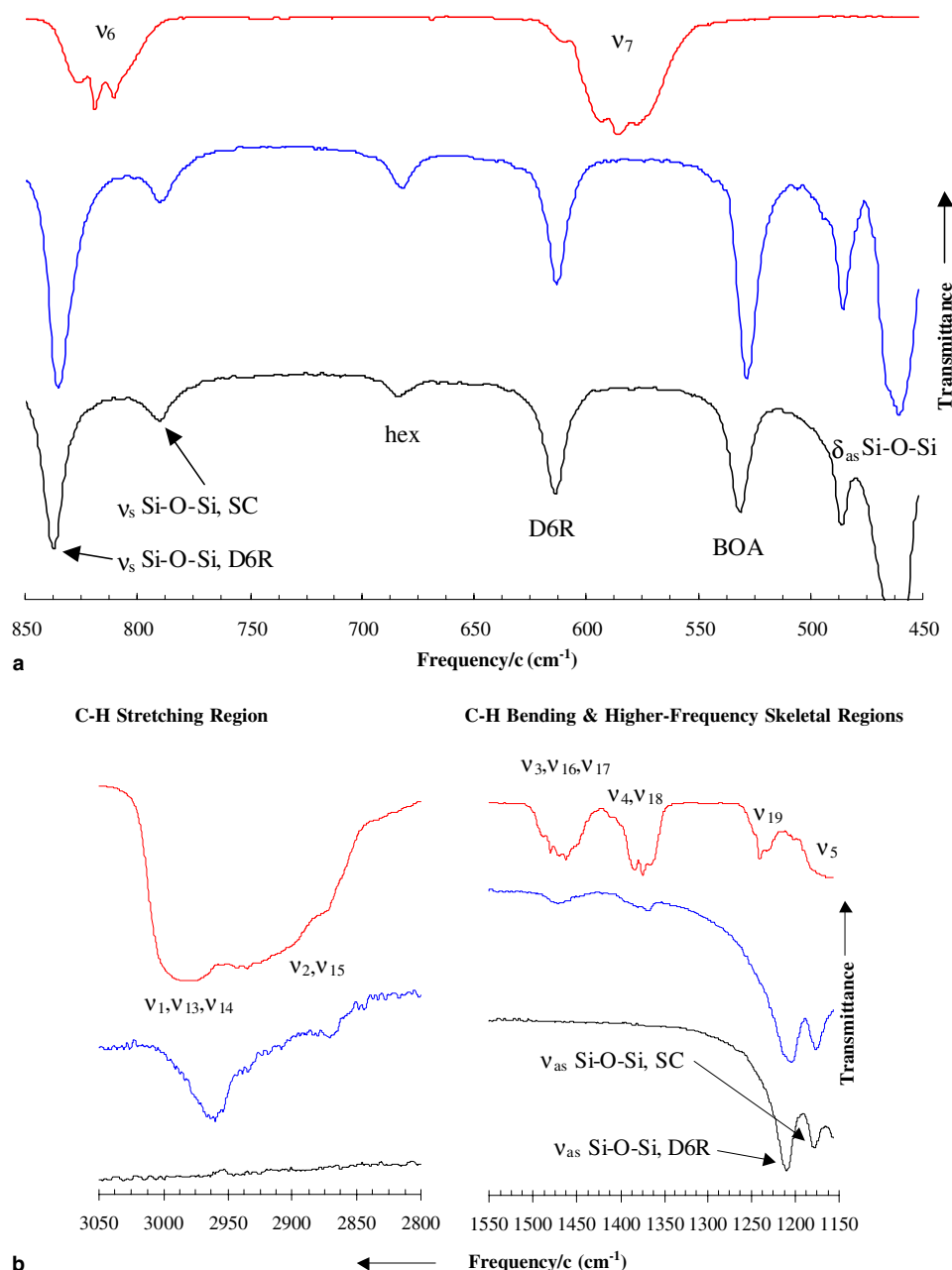


Fig. 1. Infrared vibrational spectra from gas phase TBC guest (upper, red), LAHY-included TBC (middle, blue), and the empty LAHY host (lower, black). (a) displays bands to lower frequencies from the most intense host band, while (b) displays bands to higher frequency. The ordinates for the TBC, TBC/LAHY and LAHY traces are divided by five, two, and one-and-a-half, respectively, for scaling purposes. The relative intensities of the traces in Figs. 1–3 are not strictly meaningful due to differences in scaling and presentation for purposes of expansion. The isolated guest and host bands are labeled with assignments as discussed in the text. ν_{as} = antisymmetric stretch, ν_s = symmetric stretch, δ_{as} = antisymmetric bend, SC = sodalite cage, hex = hexagonal ring channels, D6R = hexagonal prisms, BOA = (pseudo-lattice mode) bridging oxygen atoms. (For interpretation of the references to color in this figure legend, the reader is referred to the web version of this article.)

upon loading the guest into the host, are unaffected and the closest host bands at 790 cm^{-1} (sodalite Si–O–Si symmetric stretch) and 838 cm^{-1} (hexagonal prism Si–O–Si symmetric stretch) remain unaffected.

3.3. C–X stretching, CH_3 rocking and C–H bending, ν_5

The positions of the *tert*-butyl halide gas phase ν_5 bands are located at 1162 cm^{-1} (TBC), 1153 cm^{-1} (TBB), and

1147 cm^{-1} (TBI). Upon loading the guest into the host, what remains are single peaks located in the vicinity of the host Si–O–Si antisymmetric stretching band (1177 cm^{-1}) at 1176 cm^{-1} (TBC), 1173 cm^{-1} (TBB), and 1175 cm^{-1} (TBI). The 1177 cm^{-1} LAHY band is preferentially associated with sodalite cage oxygen atom motions. Fig. 5 presents an expanded view of the coalescence between the TBC C–Cl stretch/ CH_3 rocking skeletal vibrational mode ν_5 and the LAHY band arising from sodalite cage-localized Si–O–Si

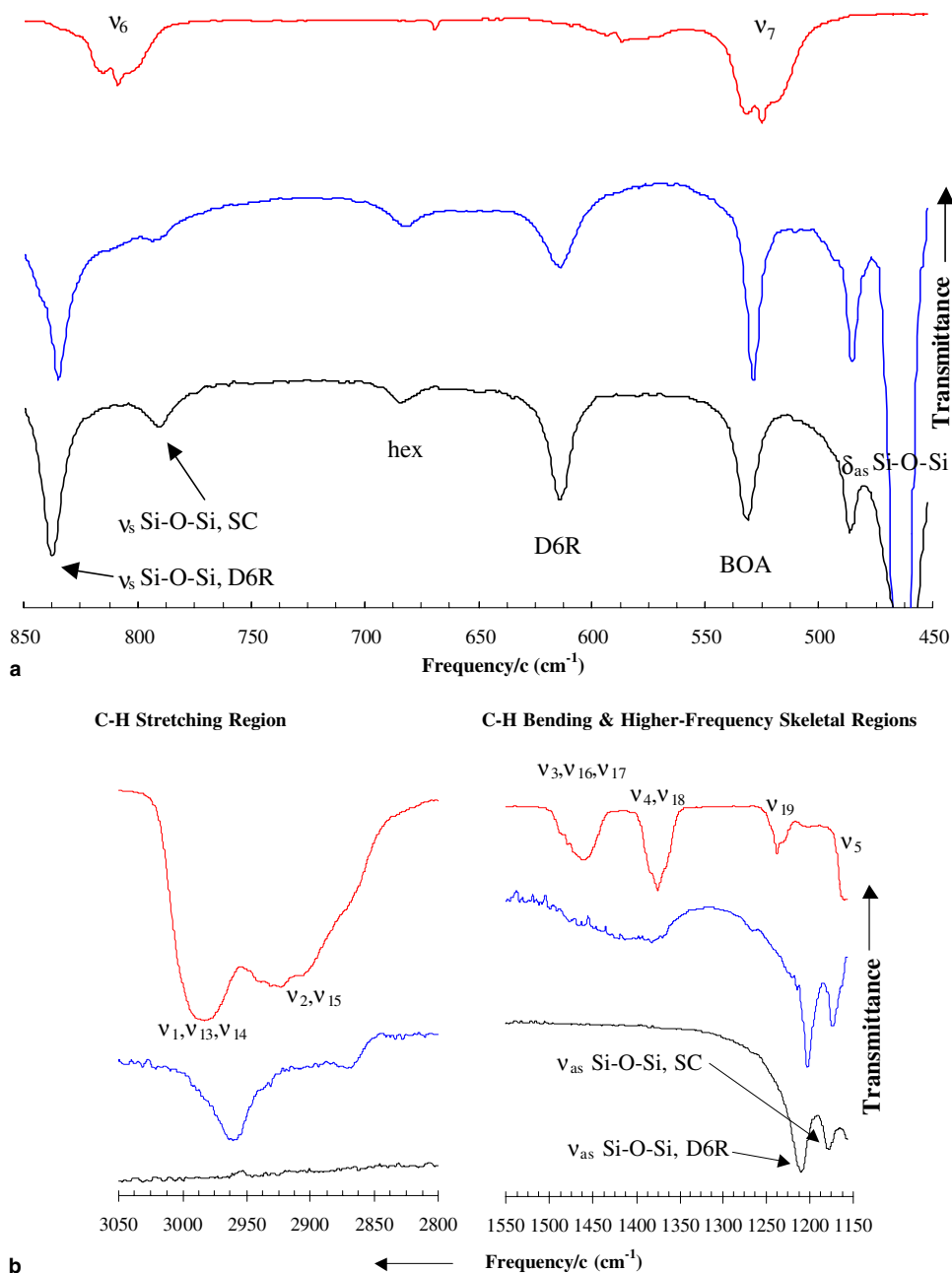


Fig. 2. Infrared vibrational spectra from gas phase TBB guest (upper, red), and from LAHY-included TBB (middle, blue), and the spectrum of the empty LAHY host (lower, black). The two-figure format is again used to display bands above and below the most intense host band. The ordinates of the TBB and LAHY traces are divided by three and one-and-a-half, respectively, for scaling purposes. The isolated guest and host bands are again labeled with assignments. (For interpretation of the references to color in this figure legend, the reader is referred to the web version of this article.)

antisymmetric stretching vibrational modes. The participating gas-phase TBB guest and the unloaded LAHY host bands are also presented.

3.4. C–C stretching and CH_3 rocking, ν_{19}

The positions of the ν_{19} guest modes shift by almost the same amounts, -28 cm^{-1} (TBC), -27 cm^{-1} (TBB), and -23 cm^{-1} (TBI), upon loading the guests into the host.

The host Si–O–Si antisymmetric stretching band at 1210 cm^{-1} remains unaffected. The 1210 cm^{-1} LAHY band is preferentially associated with hexagonal prism oxygen atom motions. Fig. 6 presents an expanded view of the coalescence between the TBB C–C stretch/ CH_3 rocking skeletal vibrational mode ν_{19} and the LAHY band arising from D6R-localized Si–O–Si antisymmetric stretching vibrational modes. The relevant bands from the participating gas-phase TBB guest and the unloaded LAHY host are shown as well.

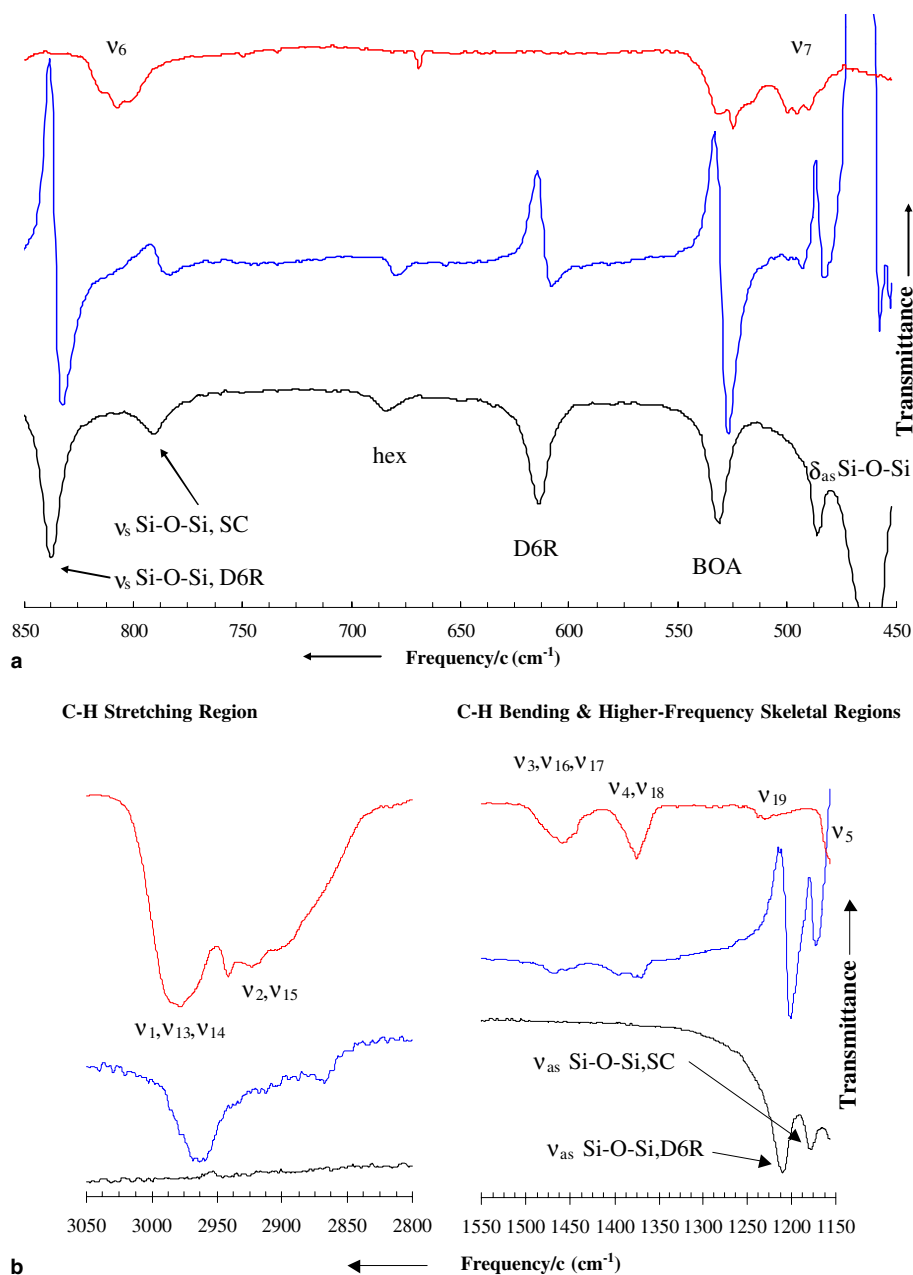


Fig. 3. Infrared vibrational spectra from gas phase TBI guest (upper, red), and from LAHY-included TBI (middle, blue), and the spectrum of the empty LAHY host (lower, black). The ordinates of the LAHY trace are divided by one-and-a-half for scaling purposes. Assignments for isolated guest and host are labeled. (For interpretation of the references to color in this figure legend, the reader is referred to the web version of this article.)

3.5. Symmetric C–H bending, $\{\nu_4, \nu_{18}\}$

The $\{\nu_4, \nu_{18}\}$ band is effectively invariant in the gas-phase spectra of the three TBH molecules, being located at $1375 \pm 1 \text{ cm}^{-1}$. The effect of TBH inclusion into LAHY on this band is pronounced, and is manifest in a different way for each of the TBH molecules. For TBC, the frequency is slightly reduced by 3 cm^{-1} . For TBB, this band merges with the TBB C–H antisymmetric bending band $\{\nu_3, \nu_{16}, \nu_{17}\}$ to form a single broad band centered at 1406 cm^{-1} that represents an increase of $+31 \text{ cm}^{-1}$ for the symmetric C–H bend. Fig. 7 presents an expanded view

of this coalescence. For TBI, the band is slightly split into two bands that are centered at 1385 cm^{-1} , which is $+10 \text{ cm}^{-1}$ from its gas-phase value.

3.6. Antisymmetric C–H bending, $\{\nu_3, \nu_{16}, \nu_{17}\}$

The $\{\nu_3, \nu_{16}, \nu_{17}\}$ band is slightly variable in gas-phase TBH, being located at $1466, 1463$ and 1460 cm^{-1} for TBC through TBI. The frequency shifts for this band upon loading TBH into LAHY are variable, with slight increases of 3 and 5 cm^{-1} for TBC and TBI, respectively. As noted in the previous section, this TBB band merges with its sym-

Table 1
Comparative summary of the characteristics of eight infrared vibrational bands of the *tert*-butyl halides (Cl, Br, and I) adsorbed in low-aluminum H-Y (LAHY) and in the gas phase

Band type and assignment	Fit parameter	TBC	TBC in LAHY ^a	Shifts ^b	TBB	TBB in LAHY ^a	Shifts ^b	TBI	TBI in LAHY ^a	Shifts ^b	Closest LAHY band
C–X stretch, ν_7	I_o	0.84	0.50	29	0.42	0.14	77	0.04	0.38	45	532 L
	$\bar{\nu}_o$ (cm ⁻¹)	584	528 L	<u>-56</u>	525	529 L	<u>4</u>	495	^c 529 G	<u>34</u>	
	$\Delta\bar{\nu}_o$ (cm ⁻¹)	17	4	-13	15	4	-11	14	8	-6	
C–C, C–X stretch, ν_6^f	I_o	0.40	–	–	0.19	–	–	0.04	–	–	838 L,
	$\bar{\nu}_o$ (cm ⁻¹)	816	^d 811	-5	808	^d 810	2	805	^d 803	-2	790 L
	$\Delta\bar{\nu}_o$ (cm ⁻¹)	16	–	–	15	–	–	14	–	–	
C–X stretch, CH ₃ rock, ν_5	I_o	1.38	0.10	-83	1.83	0.09	-40	0.46	0.09	-87	1177 G
	$\bar{\nu}_o$ (cm ⁻¹)	1162	1176 G	<u>14</u>	1153	1173	<u>20</u>	1147	^c 1175 G	<u>28</u>	
	$\Delta\bar{\nu}_o$ (cm ⁻¹)	26	10	-16	13	7	-6	14	4	-10	
C–C stretch, CH ₃ rock, ν_{19}	I_o	0.44	0.30	22	0.23	0.10	56	0.04	0.33	37	1210 G
	$\bar{\nu}_o$ (cm ⁻¹)	1235	1207 L	<u>-28</u>	1238 ^e	1203 ^e G	<u>-27</u>	1222	^c 1199 G	<u>-23</u>	
	$\Delta\bar{\nu}_o$ (cm ⁻¹)	15	15	0	13	7	-6	24	8	-16	
CH ₃ C–H symmetric bend, ν_4, ν_{18}	I_o	0.83	0.04	-53	0.68	0.04	-8	0.18	0.02	-37	1885
	$\bar{\nu}_o$ (cm ⁻¹)	1376	1373 L	<u>-3</u>	1375	^f 1406 G	<u>31</u>	1375	1385 G	<u>10</u>	
	$\Delta\bar{\nu}_o$ (cm ⁻¹)	18	26	8	14	62	48	14	28	14	
CH ₃ C–H antisymmetric bend, $\nu_3, \nu_{16}, \nu_{17}$	I_o	0.47	0.03	-28	0.34	0.04	10	0.13	0.01	-27	1885
	$\bar{\nu}_o$ (cm ⁻¹)	1466	1469 L	<u>3</u>	1463	^f 1406 G	<u>-57</u>	1460	1465 G	<u>5</u>	
	$\Delta\bar{\nu}_o$ (cm ⁻¹)	24	17	-7	22	62	40	24	20	-4	
CH ₃ C–H symmetric stretch, ν_2, ν_{15}	I_o	0.80	0.04	-51	0.56	0.02	-20	0.30	0.02	-62	3521 ^g
	$\bar{\nu}_o$ (cm ⁻¹)	2942	2872 L	<u>-70</u>	2925	2871 G	<u>-54</u>	2927	2869 L	<u>-58</u>	
	$\Delta\bar{\nu}_o$ (cm ⁻¹)	73	14	-59	56	15	-41	65	10	-55	
CH ₃ C–H antisymmetric stretch, $\nu_{11}, \nu_{13}, \nu_{14}$	I_o	1.38	0.07	-87	1.02	0.03	-35	0.42	0.04	-87	3521 ^g
	$\bar{\nu}_o$ (cm ⁻¹)	2980	2963 L	<u>-17</u>	2982	2961 L	<u>-21</u>	2976	2964 G	<u>-12</u>	
	$\Delta\bar{\nu}_o$ (cm ⁻¹)	28	18	-10	24	14	-10	28	21	-7	

The frequency of the closest host band is also given. Shifts in the frequencies of the bands are underlined for easy reference in Sections 3 and 4, which focus on the frequency shifts.

All spectra reported here are from the 1–1.5 wt% loaded faujasite in KBr wafer, versus the 1.0% unloaded faujasite in KBr wafer used for the background scan.

^a The letter after certain $\bar{\nu}_o$ values indicates the nature of the fit function that best describes the band as being either Lorentzian (L) or Gaussian (G). All gas-phase guest bands are best fit by a Gaussian lineshape function.

^b Shifts are calculated as (guest included – gas phase) so as to label the signs of the changes in the loaded LAHY spectra. Intensity shifts are in percent, relative to gas phase guest values, and are calculated using experimental intensities normalized to the maximum intensity band in each spectrum.

^c Due to the presence of derivative shapes for these bands in the loaded LAHY spectrum, this data subset derives from the fit of the band residue spectrum resulting from the scaled absorbance subtraction {“guest-included host” ± “unloaded host”}.

^d The band position is visually estimated, due to difficulties in fitting based on the position of these bands midway between the two closest host bands. Line width and intensity data for the guest-loaded host spectra were not estimated for these cases.

^e These values are for the most intense portion of the absorption bandwidth, due to asymmetry in the *P*, *Q*, *R* branch intensity distributions in the particular band of the gas-phase guest spectra.

^f The two C–H bending bands have merged to form a single, broad band.

^g These host bands are assigned to the surface Si–OH groups.

metric C–H bending band counterpart, which represents a frequency shift of -57 cm⁻¹ from the antisymmetric band’s gas-phase value (see Fig. 7).

3.7. Symmetric C–H stretching, { ν_2, ν_{15} }

In the gas phase the methyl group symmetric C–H stretching vibration band appears as a very broad, marked shoulder on the much stronger, higher-frequency antisymmetric C–H stretching band. The band positions in the gas phase are somewhat variable at 2942 cm⁻¹ (TBC), 2925 cm⁻¹ (TBB), and 2927 cm⁻¹ (TBI). This band is dramatically affected by inclusion of the guests

into LAHY. The broad nature of these bands in the gas phase is observed to diminish upon LAHY loading, with the emergence of narrow, single bands at 2872 cm⁻¹ (TBC), 2870 cm⁻¹ (TBB) and 2869 cm⁻¹ (TBI). The frequency shifts relative to the gas phase range from -70 cm⁻¹ (TBC) and -54 cm⁻¹ (TBB) to -58 cm⁻¹ (TBI).

3.8. Antisymmetric C–H stretching, { $\nu_{11}, \nu_{13}, \nu_{14}$ }

This band is also significantly affected by guest adsorption into LAHY. The gas-phase bands of the guests, the maxima of which are located at 2980 cm⁻¹ (TBC),

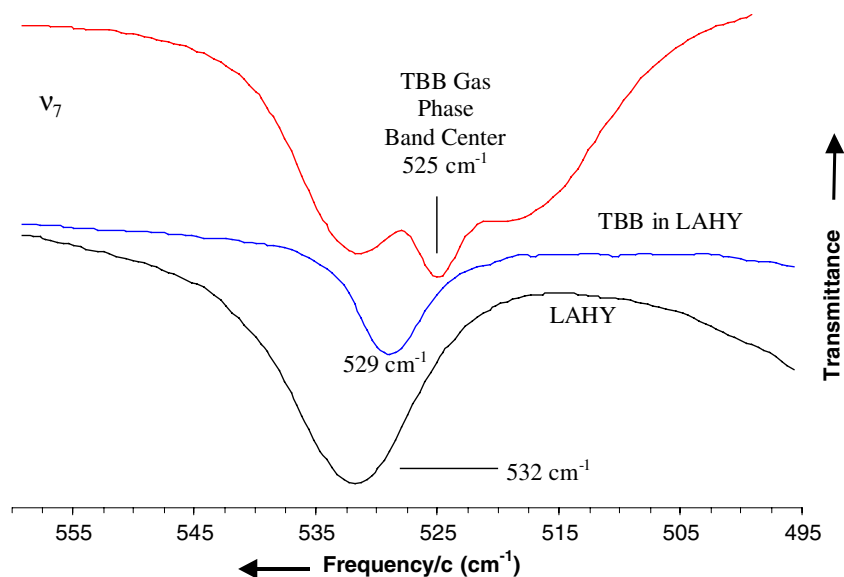


Fig. 4. An expanded view of the coalescence between the TBB C–Br stretching vibrational mode ν_7 and the LAHY band arising from D6R/S4R BOA vibrational modes (blue trace). The participating gas-phase TBB guest and the unloaded LAHY host bands are shown by the red and black traces, respectively. The relative intensities of the traces in Figs. 4–7 are not strictly meaningful, because the spectra were recorded from separate samples in different experiments. (For interpretation of the references to color in this figure legend, the reader is referred to the web version of this article.)

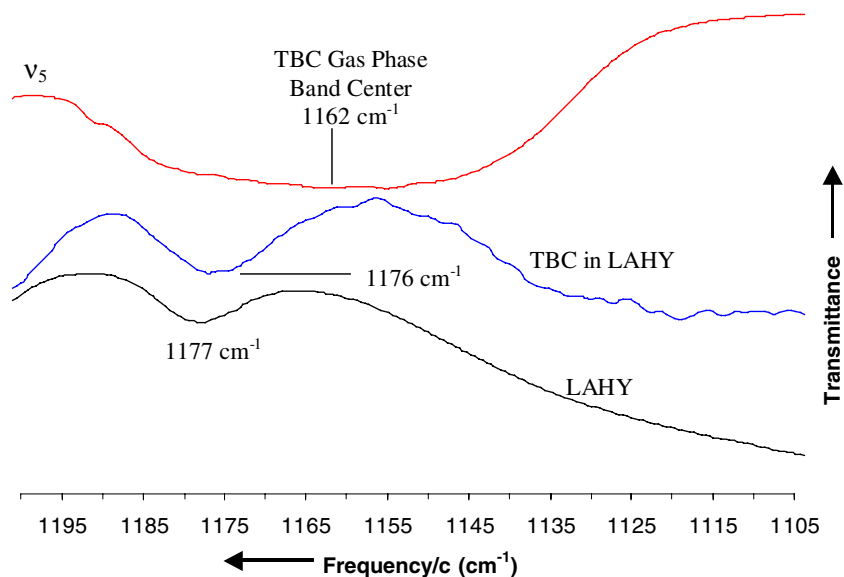


Fig. 5. An expanded view of the coalescence between the TBC C–Cl stretch/ CH_3 rocking skeletal vibrational mode ν_5 and the LAHY band arising from sodalite cage-localized Si–O–Si antisymmetric stretching vibrational modes (blue trace). The participating gas-phase TBC guest and the unloaded LAHY host bands are shown by the red and black traces, respectively. (For interpretation of the references to color in this figure legend, the reader is referred to the web version of this article.)

2982 cm^{-1} (TBB), and 2976 cm^{-1} (TBI), all move to lower frequency by -17 , -21 and -12 cm^{-1} , respectively, upon adsorption into LAHY.

4. Discussion of results

This section elaborates on the fact that in this work the TBH bands, ν_5 , ν_7 , and ν_{19} , appear to coalesce with nearby

LAHY bands upon adsorption of TBH into the host. This type of interaction was also observed in Na-X [14], where it was found to be consistent with a phonon-mediated stochastic exchange of a vibrational quantum of excitation between ν_5 and a hexagonal prism antisymmetric Si–O–Si(Al) stretching band. Moreover, members of the TBH symmetric and antisymmetric C–H bending modes are observed to coalesce with one another upon adsorption

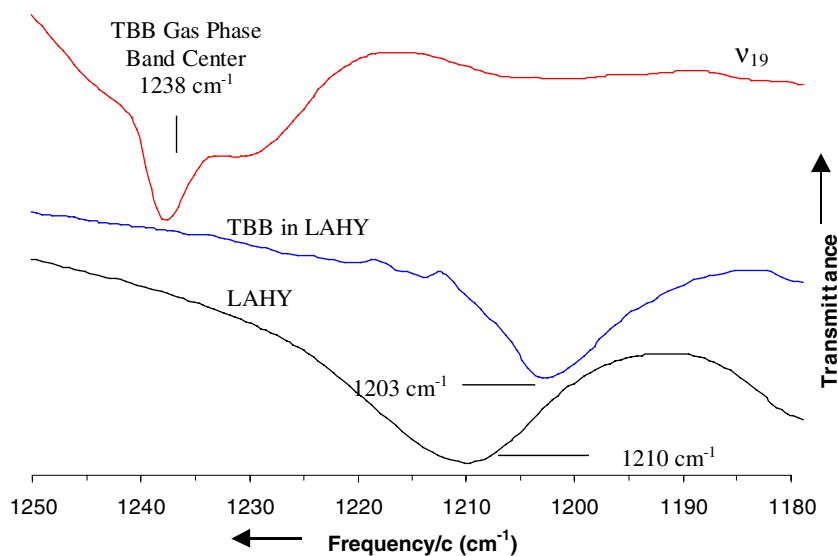


Fig. 6. An expanded view of the coalescence between the TBB C–C stretch/ CH_3 rocking skeletal vibrational mode ν_{19} and the LAHY band arising from D6R-localized Si–O–Si antisymmetric stretching vibrational modes (blue trace). The participating gas-phase TBB guest and the unloaded LAHY host bands are shown by the red and black traces, respectively. (For interpretation of the references to color in this figure legend, the reader is referred to the web version of this article.)

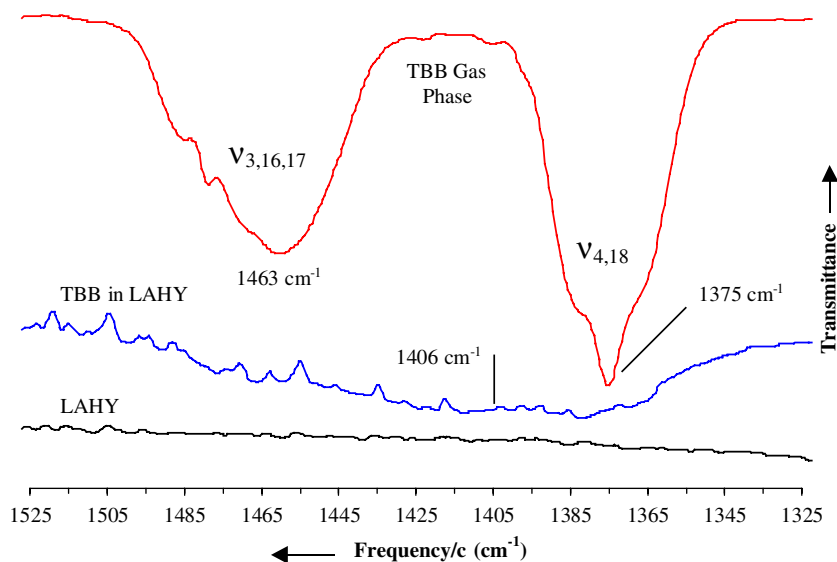


Fig. 7. An expanded view of the coalescence between the TBB antisymmetric C–H bending vibrational modes $\{\nu_3, \nu_{16}, \nu_{17}\}$ and the TBB symmetric C–H bending vibrational modes $\{\nu_4, \nu_{18}\}$ (blue trace). The participating gas-phase TBB guest bands (antisymmetric modes centered at 1463 cm^{-1} , symmetric modes centered at 1375 cm^{-1}) are shown in the red trace. The unloaded LAHY host absorption profile over this frequency range is shown as the black trace. (For interpretation of the references to color in this figure legend, the reader is referred to the web version of this article.)

of TBH into the host. The TBH C–H stretching bands show characteristics consistent with pseudo-hydrogen bonding of the methyl C–H groups, and several bands exhibit negligible changes upon adsorption of TBH into LAHY. Firstly, the assignments of the relevant LAHY host vibrational bands are briefly presented. A more thorough treatment of the assignments can be found in the [Supplementary Material](http://www.sciencedirect.com) (<http://www.sciencedirect.com>). The siting of the TBH molecules was thoroughly determined in the Na-X study. However, in order to appreciate the changes in siting that removal of the cations and adjust-

ment of framework charges makes in LAHY, the results of modeling studies of the siting of the TBH molecules are then presented. Following the modeling discussion, the guest and host band position behavior is addressed by type and discussed on a band-by-band basis. Phenomena in which a quantum of excitation is exchanged between two vibrational modes, promoted by a low-frequency lattice mode, are presented, examples of which have been observed in matrix isolation spectroscopy [19]. It was noted in early work of this kind in matrix isolation spectroscopy that the broadening of vibrational lineshapes is associated

with dephasing or loss of phase coherence of the vibration, due to the stochastic nature of the exchange process [19]. Since the guest band center frequency parameter $\bar{\nu}_0$ is of primary interest in the interpretation of interactions between the guests and host, the discussions of the FTIR results focus on the changes in frequency position of the various guest bands upon loading into LAHY.

4.1. LAHY host vibrational band assignments

Although the structure, properties and applications of X- and Y-faujasites have been extensively discussed in the literature, an unambiguous assignment of all LAHY host mid-infrared bands was not found in several searches of the chemical literature. Thus, as the first step to understanding the intermolecular interactions reported in this work, the dehydrated, unloaded LAHY spectrum was assigned [18,20–24]. Calculations of the bands were done for a better understanding of the modes. A full discussion of the assignment is given in the [Supplementary Material \(http://www.sciencedirect.com\)](http://www.sciencedirect.com). Here, only those host modes are discussed relevant to the interaction issues under consideration.

Antisymmetric Si–O–Si bending motions on the sodalite cage and hexagonal prism, respectively, are assigned to the bands at 461 and 486 cm^{-1} in comparison with like modes of Na-X, and crystalline and amorphous SiO_2 [18]. These are delocalized modes evidently favoring the indicated regions of oxygen atom displacement.

The band at 532 cm^{-1} is assigned to an LAHY pseudo-lattice mode, due to delocalized Si–O–Si bridging atom motions in both hexagonal prisms and sodalite cages, that is unique to the siliceous faujasite lattice [20–24].

The bands at 1177 and at 1210 cm^{-1} are assigned to antisymmetric stretching motions of Si–O–Si units on the sodalite cages and hexagonal prisms, respectively, on the basis of comparison with like modes in both crystalline and amorphous forms of SiO_2 [18] and Al_2O_3 . The calculations did not reproduce the frequencies very well in this region, but they do exhibit the alternating sodalite cage and hexagonal prism character of the oxygen atom motions with increasing vibrational frequency, a phenomenon that is discussed in detail in the [Supplementary Material \(http://www.sciencedirect.com\)](http://www.sciencedirect.com).

4.2. Combined guest–host modeling calculations

Modeling studies were performed in order to find the potential energy-minimized geometries of the TBH molecules in a supercage of LAHY. The Materials StudioTM simulation environment MS Modeling 3.1 (Accelrys, Inc.) was employed. First, electrostatic potential-fitted partial charges for all TBH atoms were calculated after molecular geometry optimization with a spin-restricted, gradient-corrected BLYP exchange/correlation potential using the DMol³ density functional module [25] within MS Modeling 3.1. While constraining the unit cell parameter of a single

all-silicon faujasite unit cell to the experimental LAHY value of $a = 2.43431$ nm, the geometry of the empty lattice was energy-minimized and then frozen as the template for determining the energy-minimized TBH geometry in the LAHY supercages. The Si and O atomic charges of this structure were taken from those of Jaramillo and Auerbach [26].

Several energy minima of similar geometry were found, whose energies were within less than RT of one another at 298 K. The lowest-energy geometry has the halogen atom oriented toward a pair of inward-puckered (with respect to the center of a supercage) host oxygen atoms belonging to an S4R unit of a hexagonal prism and two equatorial protons, one from each of two methyl groups, interacting with host inward-puckered oxygen atoms of another hexagonal prism S4R unit. A slightly higher-energy minimum geometry has the halogen atom interacting with three oxygen atoms of a sodalite cage S6R unit and has two equatorial protons, one from each of two methyl groups, interacting with host inward-puckered oxygen atoms of a neighboring sodalite cage S4R unit, see Fig. 8. In LAHY and at the ambient temperatures employed in these experiments, the molecules are probably moving between these two kinds of sites.

4.3. Guest–host and guest–guest exchange of a quantum of vibrational excitation

4.3.1. C–X stretching, ν_7

A careful inspection of the loaded LAHY spectra shows that there are no features to be found in the vicinity of the gas phase ν_7 frequencies. Solvent extraction of the TBH loaded X- and Y-type faujasites with subsequent nuclear magnetic resonance (NMR) experiments confirm the chemical integrity of the TBH guests in the hosts.

Thus, the possible coalescence of the guest ν_7 band with the host hexagonal prism, four-ring BOA mode is entertained. Coalescence would be the result of the stochastic exchange of a quantum of vibrational excitation between the guest and host at rates exceeding the frequency difference

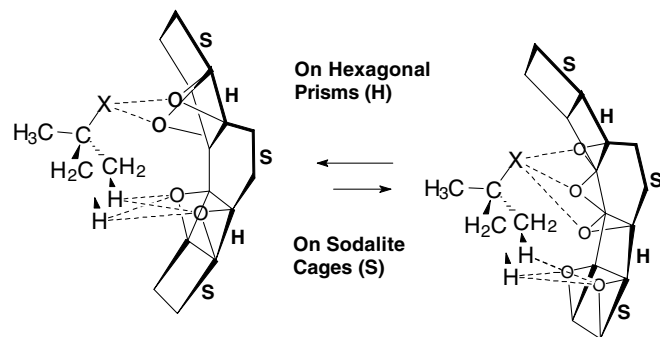


Fig. 8. Schematic of the interactions between the TBH halogen atom and an the inward-facing oxygen atoms S4R unit of a hexagonal prism and between one equatorial hydrogen atom of each of two TBH methyl groups likewise with another S4R unit adjoining the same sodalite cage.

between gas-phase guest and unloaded host bands, $52 \text{ cm}^{-1} c$ (TBC), $7 \text{ cm}^{-1} c$ (TBB), and $37 \text{ cm}^{-1} c$ (TBI), where c is the speed of light. Subsequently, frequencies will simply be given in wavenumber units with this understanding. Such a coalescence would require energy conserving, low-frequency promoting modes of these frequencies to modulate the interactions between the halogen end of the TBH molecules and the BOA atoms that point into the LAHY supercage, based on modeling studies of the siting of the TBH described above. In the study of TBH molecules in Na-X [14], a coalescence was found for ν_5 with the 1060 cm^{-1} shoulder of the host hexagonal prism antisymmetric Si–O–Si(Al) stretching band.

In the present study the locations of the coalesced bands are very near the unloaded host band, whereas the locations of the resulting band in TBH loaded Na-X is more-or-less halfway between the guest and unloaded host bands. The TBH loaded Na-X coalescence was, thus, treated as an exchange of a vibrational quantum between the guest vibrational mode and one host vibrational mode. NMR studies have been done on solution intermolecular proton exchange line coalescence between the chemical shifts of two different chemical species [27]. These phenomena were shown to obey a mole fraction-weighted law of chemical exchange [27]. If several host oscillators for every TBH ν_7 mode were involved in the vibrational quantum excitation exchange, this could afford an explanation for finding a coalesced band near the unloaded host frequency.

The corresponding form of the weighted exchange in the current vibrational context would be

$$\nu_{\text{obs}} = \nu_7 \chi_{\nu_7} + \nu_{\text{BOA}} \chi_{\text{BOA}}, \quad (1)$$

where ν_i are the oscillator frequencies and χ_i are the fractions of the guest, $i = \nu_7$, and bridging oxygen atom modes, $i = \text{BOA}$, (532 cm^{-1}). Note that for a given pair of exchange partners, the observed frequency from Eq. (1) will depend only on the relative amounts of exchanging species.

Eq. (1) has been fitted to the data for TBB and TBI, omitting TBC for the moment, whose coalesced line appears to lie below the range spanned by the gas-phase guest frequency and host BOA mode. The result gives a value of 36.9 ± 15.9 effectively degenerate host BOA modes per supercage.

Although the uncertainty in this value is high due to the dependence on the relatively inaccurate difference between the unloaded host frequency and the coalesced lines, it is believed that the reasonableness of the result is strong evidence for the qualitative nature of the vibrational quantum excitation exchange. Consider that the number of bridging oxygen atoms located on the surface of a supercage is 48. Of these oxygen atoms, twelve (12) are directed in towards the centers of hexagonal prisms or sodalite cages, with the remaining 36 directed into the supercage with which a TBH molecule could interact. Thus, there are 36 inward directed framework oxygen atoms that may support a BOA mode. Therefore

36.9 ± 15.9 effectively degenerate, host BOA modes per supercage does not seem to be unreasonable for a vibrational quantum exchange phenomenon.

Such a vibrational quantum exchange phenomenon was not observed for the TBH ν_7 mode in Na-X, because the host modes are at appreciably different frequencies [19] and the juxtaposition of guest and host modes was evidently not favorable to an exchange coalescence. Other reasons for differences between the TBH/Na-X and TBH/LAHY systems will be encountered in connection with other bands.

Why the TBC/LAHY line coalesces slightly to the low-frequency side of the unloaded LAHY and evades successful fitting is not clear. As stated previously, the actual frequency differences do not greatly exceed the uncertainties in the peak positions. Taking this into account, TBC may be viewed to be as much an example of the quantum exchange phenomenon as TBB and TBH. It is possible that additional exchange phenomena with host modes lower in frequency than the BOA modes, such as the hexagonal prism 486 cm^{-1} and/or the sodalite cage 461 cm^{-1} antisymmetric bending modes, may be playing a role. These host modes do have displacements of O atoms shown to be interacting with TBC at its sites in the supercage.

The applicability of Eq. (1) is subject, in principle, to further experimental testing by means of a study of coalesced band position as a function of guest loading and by means of the temperature dependence of the degree of coalescence and of the coalesced band width. However, the fact that the current results for TBB and TBI can be modeled in a reasonable way by this simple relationship is interesting and encouraging.

Low frequency, energy conserving, promoting modes below 100 cm^{-1} are required. In low-temperature IR and Raman studies [27] of X- and Y-faujasites, SiO_4 “rotational” modes were observed near 100 cm^{-1} . However, aside from acoustic lattice modes, the only modes identified below 100 cm^{-1} were cation modes. As there are essentially no cations present in LAHY, one can only entertain crystal lattice modes or TBH molecular diffusional motions between sites of similar character but with energy differences of the required order of energy.

4.3.2. C–X stretching, CH_3 rocking, and C–H bending, ν_5

The band assigned to the very intense skeletal mode ν_5 (A_1) near 1150 cm^{-1} in the guests is a superposition of C–X stretching, CH_3 rocking and mostly methyl axial H atom displacements in the xy plane of the molecule. Like ν_7 , inspection of the host–guest spectra in the vicinity of the gas-phase ν_5 frequencies shows that the guest ν_5 bands are nowhere to be found. However, in place of the somewhat sodalite cage-localized, host Si–O–Si antisymmetric stretching (SOSAS) band at 1177 cm^{-1} , at a small shift is found a new peak, 1176 cm^{-1} (TBC), 1173 cm^{-1} (TBB), and 1175 cm^{-1} (TBI). The observation of a guest–host hybrid band that is intermediate between the isolated guest and host frequencies and near the unloaded host band

again suggests an exchange of a quantum of vibrational excitation between the guest and host. Application of the weighted exchange expression in Eq. (2) gives agreement with

$$\nu_{\text{obs}} = \nu_{\text{v5}}\chi_{\text{v5}} + \nu_{\text{SOSAS}}\chi_{\text{SOSAS}} \quad (2)$$

TBH-LAHY band positions (predicted values are 1174 cm^{-1} , 1173 cm^{-1} , and 1172 cm^{-1} and observed values are 1176 cm^{-1} , 1173 cm^{-1} , and 1175 cm^{-1} for TBC through TBI, respectively). The number of effectively degenerate Si–O–Si antisymmetric stretching modes per molecule of TBH, 35.8 ± 11.2 is again not unreasonable in terms of the 36 oxygen atoms pointing into the supercage, whose sodalite cage Si–O–Si antisymmetric stretching modes could interact and exchange vibrational excitation with the TBH molecules. Such a coalescence would require energy conserving, low-frequency promoting modes of frequencies, 15 cm^{-1} (TBC), 24 cm^{-1} (TBB), and 30 cm^{-1} (TBI), to modulate the interactions between the halogen end of the TBH molecules and the O atoms that point into the LAHY supercage, based on modeling studies of the siting of the TBH to be described subsequently. As discussed above for ν_7 , these promoting modes would seem to be either crystal lattice modes or site-to-site diffusional motions of the TBH molecule.

4.3.3. C–C stretching and CH_3 rocking, ν_{19}

The normal coordinate analysis of ν_{19} (E) shows that this vibrational mode is skeletal and is best pictured as a superposition of mostly C–C stretching with CH_3 rocking displacements. Like ν_5 and ν_7 , inspection of the host–guest spectra in the vicinity of the gas-phase ν_{19} frequencies shows that the guest ν_{19} bands are nowhere to be found. However, in place of the host hexagonal prism Si–O–Si symmetric stretching (SOSSS) band at 1210 cm^{-1} , at a small shift is found a new peak, 1207 cm^{-1} (TBC), 1207 cm^{-1} (TBB), and 1199 cm^{-1} (TBI). Again, the proximity of ν_{19} to the SOSSS band would seem to suggest an exchange of a quantum of vibrational excitation between the guest and host. However, since the bands of TBH-loaded LAHY lie below the frequency range between the gas-phase ν_{19} band and the unloaded host band, the application of the analog of Eqs. (1) and (2) is not possible. Nevertheless, along the lines discussed above for the behavior of the TBC ν_7 band in LAHY, a degree of quantum exchange with host bands at lower frequency, such as the sodalite cage SOSAS band at 1177 cm^{-1} , may draw the frequency below that of the hexagonal prism 1210 cm^{-1} SOSSS band. In this case energy conserving, low-frequency promoting modes of 25 cm^{-1} (TBC), 24 cm^{-1} (TBB), and 12 cm^{-1} (TBI) would be required to modulate the interactions between the halogen end of the TBH molecules and the O atoms that point into the LAHY supercage, based on modeling studies of the siting of the TBH to be described subsequently. As described previously, these would seem to be either crystal lattice modes or site-to-site diffusional motions of the TBH molecule.

One might ask why there are so many participating host modes in the three vibrational excitation exchange phenomena in LAHY, discussed above, whereas in the single example of excitation exchange for TBH molecules in Na-X [14], and in the TBB C–H bending coalescence described below, there appears to be more-or-less one host and one guest mode involved. Strong guest–host interactions, such as are found in Na-X, could destroy the degeneracy of the host modes, thereby making guest–host exchange with only a few split-off members of the former band a possibility, as illustrated in Fig. 9. On the other hand, weak guest–host interactions, such as are present in LAHY, may leave the band essentially intact, making it possible for many effectively degenerate host modes to participate in the exchange, also illustrated in Fig. 9.

4.4. TBB antisymmetric and symmetric C–H bending band members

As indicated below, the relatively weak coupling of the TBB methyl group C–H bending motion to the host appears to serve to coalesce a member of the antisymmetric C–H bending band at 1463 cm^{-1} in the gas phase, per ~ 1.8 members of the symmetric C–H bending band at 1375 cm^{-1} in the gas phase, to an intermediate 1406 cm^{-1} band in LAHY. The ratio of the numbers of modes is again based, according to the weighted exchange principle, on the coalesced band position 31 cm^{-1} above the gas phase TBB symmetric C–H bending frequency and 57 cm^{-1} below the TBB antisymmetric C–H bending frequency.

Additional evidence for the vibrational energy quantum exchange phenomenon is the broadening of the coalesced

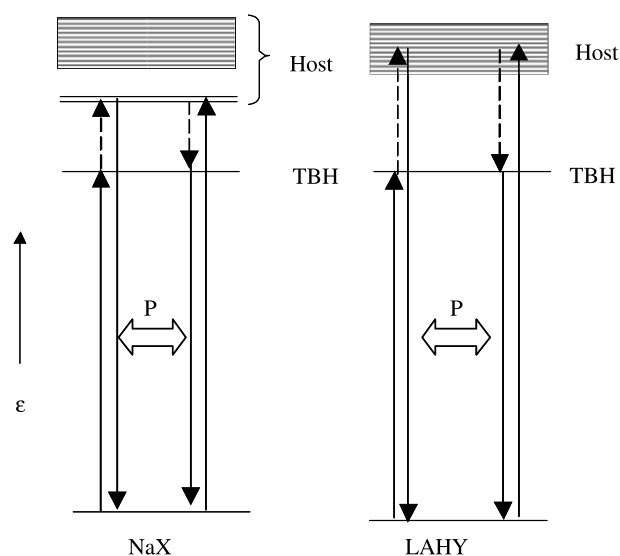


Fig. 9. Schematic diagram illustrating the excitation energies of a TBH guest vibration, split-off excitation energies from the host Na-X band under strong guest–host interaction conditions, and the main Na-X and LAHY vibrational bands. Also shown are the proposed excitation exchange processes between TBH guest and Na-X and LAHY hosts, with the exchanging quanta in solid arrows and the energy-conserving promoting modes in dotted arrows. P indicates the rate of exchange.

line, $\Delta\bar{\nu}_0 = 62 \text{ cm}^{-1}$, relative to the gas phase TBB symmetric C–H bend linewidth, $\Delta\bar{\nu}_0 = 14 \text{ cm}^{-1}$ and antisymmetric C–H bending linewidth, $\Delta\bar{\nu}_0 = 22 \text{ cm}^{-1}$. For a simple, equally-weighted, two-member mode of the kind used in the exchange phenomenon in Na-X [14], the frequency difference of $1463 - 1375 = 88 \text{ cm}^{-1}$ and the linewidth of 62 cm^{-1} would correspond to a quantum exchange frequency of at least $4.68 \times 10^{11} \text{ s}^{-1}$ (equivalent to 15.6 cm^{-1}) plus an additional 46.4 cm^{-1} or less of heterogeneous broadening. This line was actually best fit by a Gaussian, also suggesting the presence of a degree of heterogeneous broadening. The exchange requires promoting modes of 88 cm^{-1} . This magnitude of promoting mode may be provided by SiO_4 “rotation” modes or by site-to-site diffusional motion of the TBH molecule. This phenomenon has been reported in matrix isolation spectroscopy [19].

4.5. Bands unaffected by guest–host interactions

4.5.1. C–C and C–X stretching, ν_6

The atomic displacements during the course of the vibration ν_6 (A_1) are best described as a skeletal mix of C–C stretch, with a smaller amount of C–X stretching motion. Thus, the halogen–oxygen interaction indicated in the molecular modeling perturbs this molecular mode of motion relatively little. Also, the axial methyl group displacement is minimal, while considerable equatorial methyl group H displacement predominates. Although this mode has significant equatorial methyl group H atom displacement, one does not expect the C–H bending motion to greatly affect the guest host interaction, being an atomic motion that is largely normal to the direction of the guest–host oxygen atom interaction.

4.5.2. Symmetric C–H bending $\{\nu_4, \nu_{18}\}$

The CH_3 group symmetric C–H bending band at 1375 cm^{-1} in the gas-phase guest spectra contains contributions from the two normal modes ν_4 (A_1) and ν_{18} (E). These modes remain unaffected by loading of TBH into LAHY, except for the case of TBB. In this case a portion of the two modes remains unaffected, while, as described above, a portion of the band coalesces with a counterpart from the antisymmetric C–H bending band. Clearly the modeling calculations show that only the equatorial methyl H atom interacts with the host supercage oxygen atoms of the S4R. However, one does not expect the C–H bending motion to greatly affect the guest host interaction, being an atomic motion that is largely normal to the direction of the guest–host oxygen atom interaction.

4.5.3. Antisymmetric C–H bending $\{\nu_3, \nu_{16}, \nu_{17}\}$

The antisymmetric CH_3 C–H bending band located at $1463 \pm 3 \text{ cm}^{-1}$ in gas-phase TBH is a superposition of the C–H bending normal modes ν_3 (A_1), ν_{16} (E) and ν_{17} (E). These modes are antisymmetric in the sense that one of the methyl hydrogen atoms moves spatially out of phase with respect to the other two. These modes remain unaf-

ected by loading of TBH into LAHY, except for the case of TBB. In this case a portion of the two modes remains unaffected, while, as described above, a portion of the band coalesces with a counterpart from the symmetric C–H bending band. Clearly the modeling calculations show that only the equatorial methyl H atom interacts with the host supercage oxygen atoms of the S4R. However, one does not expect the C–H bending motion to greatly affect the guest host interaction, being an atomic motion that is largely normal to the direction of the guest–host oxygen atom interaction.

4.6. Non-coalescent bands strongly affected by guest–host interactions

4.6.1. TBH symmetric C–H stretch, $\{\nu_2, \nu_{15}\}$

The TBH bands all more or less uniformly shift to lower frequency by substantial amounts of $54\text{--}70 \text{ cm}^{-1}$ upon adsorption into LAHY. No host bands exist in this region, and not surprisingly no concomitant host band shifts are observed. The effects are consistent with pseudo-hydrogen bonding of the equatorial methyl protons to the S4R oxygen atoms of the supercage predicted in the modeling study.

4.6.2. Antisymmetric C–H stretching, $\{\nu_1, \nu_{13}, \nu_{14}\}$

The TBH antisymmetric C–H stretching bands likewise all more or less uniformly shift to lower frequencies by smaller amounts of $12\text{--}21 \text{ cm}^{-1}$ upon adsorption into LAHY. Again no host effects are expected or observed. The band effects are also consistent with pseudo-hydrogen bonding, as described for the symmetric C–H stretch. However, the antisymmetric nature of the stretching may tend to diminish the net pseudo-hydrogen bonding effect in comparison with the effect on the symmetric stretch.

5. Summary

Room-temperature FTIR spectra of *tert*-butyl halide (TBH) loaded into low-aluminum H-Y zeolite (LAHY) were obtained and analyzed. Three types of phenomena were observed: (1) four bands exhibited evidence of an exchange of a vibrational excitation quantum between guest and host or between two different modes of the guest; (2) TBH guest bands whose behavior indicates pseudo-hydrogen bonding between oxygen atoms of the LAHY host pointing into the supercage and TBH methyl group hydrogen atoms; and (3) TBH guest bands that were essentially unaffected by guest–host interactions. The particular host modes responsible for promoting exchange and for ensuring energy conservation, along with particular modes exhibiting pseudo-hydrogen bonding are rationalized in terms of the siting of the TBH guest in the LAHY host supercage. Modeling studies consistent with the rationalization point to the TBH halide atom interacting with the oxygen atoms of the four-membered rings of the LAHY hexagonal prisms pointing into the supercage. Concurrently, the equatorial H atoms, one on each of two TBH methyl groups, also inter-

act with the inward-facing oxygen atoms of the four-membered rings of the LAHY hexagonal prisms.

Acknowledgments

The author thanks Professor David C. Doetschman of Binghamton University (State University of New York) for countless invaluable discussions regarding the results of this work and their interpretation. The author would also like to thank Dr. Szu-Wei Yang, Charles Kanyi, Barry Jones and Chrispin Kowenje of Binghamton University (State University of New York) for many helpful discussions regarding the results of this work. The generous hospitality of Dr. Donald P. Wyman, Sr. Vice President and Director of Research and Development for Rochester Midland Corporation, is greatly appreciated for helpful discussion and for allowing the time necessary to conduct and complete this work. The author would also like to acknowledge one of the referees of this manuscript for drawing his attention to similar phenomena in matrix isolation spectroscopy [19].

Appendix A. Supplementary data

Supplementary data associated with this article can be found, in the online version, at [doi:10.1016/j.chemphys.2005.12.024](https://doi.org/10.1016/j.chemphys.2005.12.024).

References

- [1] D. Breck, *Zeolite Molecular Sieves*, Wiley, New York, 1974.
- [2] J. Sivaguru, T. Poon, R. Franz, S. Jockusch, W. Adam, N. Turro, *J. Am. Chem. Soc.* 126 (2004) 10816.
- [3] J. Hriljac, M. Eddy, A. Cheetham, J. Donohue, G. Ray, *J. Solid State Chem.* 106 (1993) 66.
- [4] L. Bull, A. Cheetham, B. Powell, J. Ripmeester, C. Ratcliffe, *J. Am. Chem. Soc.* 117 (1995) 4328.
- [5] L. Bull, M. Henson, A. Cheetham, J. Newsam, S. Heyes, *J. Phys. Chem.* 97 (1993) 11776.
- [6] G. Vitale, C. Mellot, A. Cheetham, *J. Phys. Chem. B* 101 (1997) 9886.
- [7] S. Hashimoto, S. Ikuta, T. Asahi, H. Masuhara, *Langmuir* 14 (1998) 4284.
- [8] J. Kneller, T. Pietraß, K. Ott, A. Labouriau, *Micropor. Mesopor. Mater.* 62 (2003) 121.
- [9] C. Mellot, A. Cheetham, *J. Phys. Chem. B* 103 (1999) 3864.
- [10] I. Halasz, S. Kim, B. Marcus, *J. Phys. Chem. B* 105 (2001) 10788.
- [11] Y. Huang, J. Leech, H. Wang, *J. Phys. Chem. B* 107 (2003) 7632.
- [12] Y. Huang, J. Leech, *J. Phys. Chem. B* 107 (2003) 7647.
- [13] Y. Huang, H. Wang, *Langmuir* 19 (2003) 9706.
- [14] J. Fox, A. Meenakshi, *J. Phys. Chem. B* 109 (2005) 9917.
- [15] R. Borkowski, D. Doetschman, J. Fox, C. Gargossian, *Solid State Ionics* 100 (1997) 95.
- [16] M. Stimson, M. O'Donnell, *J. Am. Chem. Soc.* 74 (1952) 1805.
- [17] D. Gupta, L. Wang, L. Hanssen, J. Hsia, R. Datta, *NIST Special Publication No. 260–122* (1998) SRM 1921.
- [18] C. Craver (Ed.), *The Coblenz Society Desk Book of Infrared Spectra*, second ed., Coblenz Society, Kirkwood, MO, USA, 1982, p. 471.
- [19] B. Swanson, L. Jones, in: J. Durig (Ed.), *Vibrational Spectra and Structure*, vol. 12, Elsevier Scientific, New York, 1983 (Chapter 1).
- [20] C. Blackwell, *J. Phys. Chem.* 83 (1979) 3257.
- [21] A. deMan, R. van Santen, *Zeolites* 12 (1992) 269.
- [22] E. Flanigen, H. Khatami, H. Szymanski, *Adv. Chem. Ser.* 101 (1971) 201.
- [23] A. Rodriguez, *Vib. Spectrosc.* 9 (1995) 225.
- [24] W. Mozgawa, *J. Mol. Struct.* 596 (2001) 129.
- [25] B. Delley, *J. Chem. Phys.* 113 (2000) 7756; B. Delley, *J. Chem. Phys.* 92 (1990) 508.
- [26] E. Jaramillo, S. Auerbach, *J. Phys. Chem. B* 103 (1999) 9589.
- [27] E. Schulman, D. Dwyer, D. Doetschman, *J. Phys. Chem.* 94 (1990) 7308.